Separation Science and Technology
Publication details, including instructions for authors and subscription information:
http://www.informaworld.com/smpp/title~content=t713708471

Transport Phenomena in Zonal Centrifuge Rotors. VI11. Dispersion in Reorienting Gradient Systems

H. W. Hsu[a]
[a] DEPARTMENT OF CHEMICAL AND METALLURGICAL ENGINEERING, THE UNIVERSITY OF TENNESSEE, KNOXVILLE, TENNESSEE

To cite this Article Hsu, H. W.(1973) 'Transport Phenomena in Zonal Centrifuge Rotors. VI11. Dispersion in Reorienting Gradient Systems', Separation Science and Technology, 8: 5, 537 — 549
To link to this Article: DOI: 10.1080/00372367308057044
URL: http://dx.doi.org/10.1080/00372367308057044

SEPARATION SCIENCE, 8(5), pp. 537-549, 1973

Transport Phenomena in Zonal Centrifuge Rotors. VIII. Dispersion in Reorienting Gradient Systems

H. W. HSU

DEPARTMENT OF CHEMICAL AND METALLURGICAL ENGINEERING
THE UNIVERSITY OF TENNESSEE
KNOXVILLE, TENNESSEE 37916

Abstract

Reorienting dispersion in zonal gradient rotors is analytically investigated by evaluating the change of surfaces in each isodense layer. Analytical expressions for isodense surfaces at various levels were obtained as a function of the rotational speed and the ratio of rotor configurations, height of rotor to inside radius of rotor, and outside radius of rotor core to inside radius of rotor. Characteristics of the changes of each isodense layer were computed from the formula derived. It is also shown that control of rotor acceleration and deceleration is unnecessary. The dispersion due to gradient reorientation is a constant for a given rotor with a given loading level.

INTRODUCTION

The early mathematical analysis of the area of isodensity surfaces in reorienting gradient systems (*1*) has been extended to a rotor with core but without septa configuration. In the previous paper (*1*) we concluded that one has to bring the rotor as slowly as possible up to a pseudo-steady-state rpm, the minimum rpm at which the isodense paraboloid will stop changing its shape with an increase of rpm; then after this speed is reached, the rate of acceleration of the rotor does not appreciably affect the shearing forces in the liquids. Because no further variation of interfacial area occurs, dispersion due to the shearing forces in each layer disappears.

The present analysis shows that the previous conclusion was incorrect. We would like to point out that the dispersion of sample layers in centrifugation is independent of the rate of acceleration in the startup of a rotor. The dispersion of sample layers (the resolution) depends on the configuration of a rotor and loading levels. With a given rotor at a given loading level, a loss or resolution due to dispersion from the changes of interfacial area is a constant. For K-III and J-I rotors, those dispersion constants have been evaluated analytically.

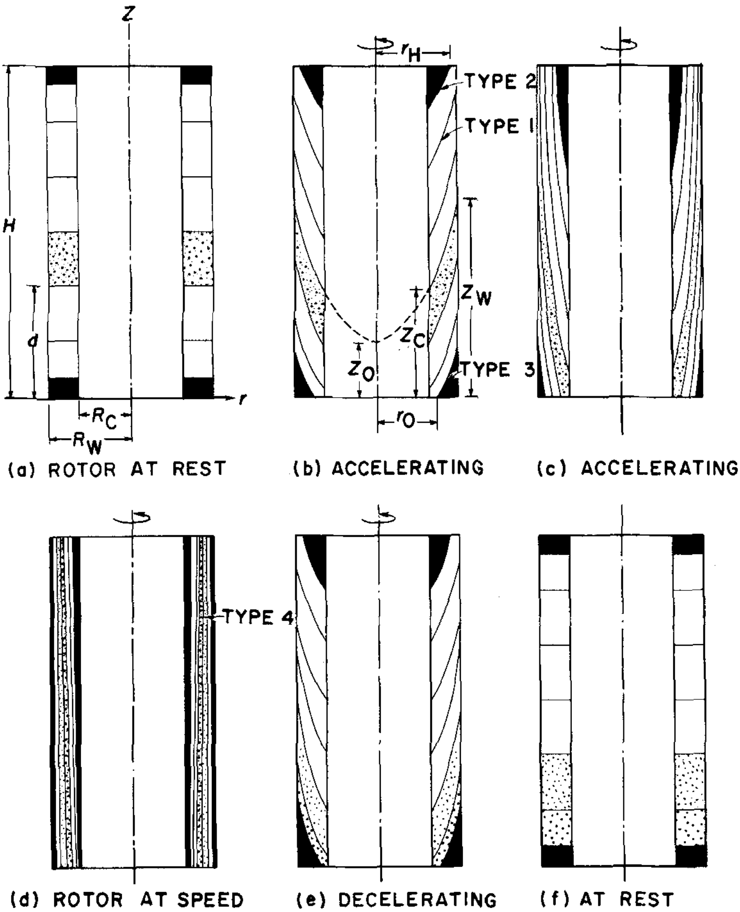

FIG. 1. Schematic diagram of reorienting gradient rotor with core.

FORMULATION OF PROBLEM

We consider a cylindrical rotor system with inside rotor wall radius R_w, outer core radius R_c, and height H. The rotor is filled, at rest, with density gradient and sample layer as shown schematically in Fig. 1a. Then the rotor is set to accelerate to a given rotational speed. During acceleration, each isodense surface becomes part of a paraboloid of revolution and can go through a series of configurations. There are four types of paraboloid configurations which will occur, depending on the liquid loading level and change in angular velocity. They are shown in Figs. 1b and 1d as Types 1, 2, 3, and 4:

$$\text{Type 1: } Z_c > 0,\ r_H = R_w, \text{ and } Z_w < H$$

$$\text{Type 2: } Z_c > 0,\ r_H < R_w, \text{ and } Z_w = H$$

$$\text{Type 3: } Z_c < 0,\ r_H = R_w, \text{ and } Z_w < H$$

$$\text{Type 4: } Z_c < 0,\ r_H < R_w, \text{ and } Z_w = H$$

where Z_c and Z_w are the heights at the intersection of the paraboloid with the rotor outer core and the inside rotor wall, respectively.

The sample layer sediments through the reoriented gradient while the rotor is at speed. The separated particles band in respective isodensity zones. Figures 1c and 1d are schematic diagrams of the reorienting gradient rotor system in acceleration and the rotor at speed, before the particles have sedimented appreciably and after sedimentation banding in respective isodensity zones. The distribution during deceleration is shown in Fig. 1e, with the distribution at rest shown in Fig. 1f. The separated zones are recovered by draining the gradient out the bottom of the rotor or by displacing it out the top.

MATHEMATICAL FORMULAS FOR ISODENSITY SURFACES

The equation describing the parabolic surface of revolution is well known and is given by Bird et al. (*2*) as

$$Z = \frac{\omega^2 r^2}{2g} + Z_0 \tag{1}$$

where Z is a vertical axial coordinate, r is a radial coordinate as shown in Fig. 1a, ω is an angular velocity, g is gravitational force, and Z_0 is the minimum of Z in the paraboloid, which depends on the angular velocity and the loading level of liquid. For a rotor with core, Z_0 is a hypothetical point which lies inside the core and changes from positive to negative with an increase in angular velocity, ω, or decrease in loading level. The equation describing the paraboloid interfacial area can be obtained from Eq. (1) to give

$$S_i = \int_l^u r\left[1 + \left(\frac{dr}{dZ}\right)^2\right]^{1/2} dZ$$

$$= \frac{2\pi g}{\omega^2}\int_l^u \left[\frac{2\omega^2}{g}(Z - Z_0) + 1\right]^{1/2} dz \quad (2)$$

The quantities l and u are the lower and upper integration limits. These values depend on the paraboloid configuration and must be constrained by the volume of liquid loaded. The constrained liquid volumes in the paraboloid for configuration Types 1 and 2 are

$$V = \pi(R_w^2 - R_c^2)\cdot\alpha H = \pi\cdot(R_w^2 - R_c^2)\cdot Z_c + \pi\int_{Z_c}^{Z_w}(R_w^2 - r^2)\,dZ \quad (3a)$$

and

$$V = \pi(R_w^2 - R_c^2)\cdot\alpha H = \pi(R_w^2 - R_c^2)\cdot Z_c + \pi\int_{Z_c}^{H}(R_w^2 - r^2)\,dZ \quad (3b)$$

respectively. For Types 3 and 4, they are

$$V = \pi(R_w^2 - R_c^2)\cdot\alpha H = \pi\int_0^{Z_w}(R_w^2 - r^2)\,dZ \quad (3c)$$

and

$$V = \pi(R_w^2 - R_c^2)\cdot\alpha H = \pi\int_0^{H}(R_w^2 - r^2)\,dZ \quad (3d)$$

respectively. The quantity $\alpha = d/H$ in Eqs. (3) is the liquid loading level as shown in Fig. 1a. One may visualize from Fig. 1b that if $u = H$, the meaningful limit is r_H, the radius of an isodense paraboloid at the upper wall of a rotor; if $l = 0$, the meaningful limit is r_0; the radius of an isodense paraboloid at the bottom wall of a rotor. Thus it is more convenient to express Eq. (2) in terms of a radial variable instead of a height variable.

If we define the following reduced variables,

$$\alpha = d/H \quad (4a)$$

$$\beta = R_c/R_w \quad (4b)$$

$$\gamma = H/R_w \tag{4c}$$

$$\rho_H = r_H/R_w \tag{4d}$$

$$\rho_0 = r_0/R_w \tag{4e}$$

$$\zeta_c = Z_c/R_w \tag{4f}$$

$$\zeta_0 = Z_0/R_w \tag{4g}$$

$$\Omega = \omega^2 R_w/g \tag{4h}$$

$$A_i = S_i/\pi(R_w^{\ 2} - R_c^{\ 2}) \tag{4i}$$

We obtain the reduced isodensity surface area for each type of configuration together with its constrained specifications as follows:

Type 1: $0 < \zeta_c < \gamma$, $\rho_H = 1$

$$A_1 = \frac{2}{3\Omega^2(1-\beta^2)}[(1+\Omega^2)^{3/2} - (1+\Omega^2\beta^2)^{3/2}] \tag{5}$$

with constraints

$$\zeta_c = \alpha\gamma - \frac{\Omega}{4}(1-\beta^2) > 0 \tag{5a}$$

and

$$\rho_H = \left[\frac{2(1-\alpha)\gamma}{2} + \frac{1+\beta^2}{2}\right]^{1/2} > 1 \tag{5b}$$

One will see that for this type $u = Z_w$, and the term of $(Z - Z_0)$ at Z_w can be obtained from Eq. (1) to give

$$(Z_w - Z_0) = \frac{\omega^2 R_w^{\ 2}}{2g} \tag{5c}$$

Type 2: $0 < \zeta_c < \gamma$, $\beta < \rho_H < 1$

$$A_2 = \frac{2}{3\Omega^2(1-\beta^2)}[(1+\Omega^2\rho_H^{\ 2})^{3/2} - (1+\Omega^2\beta^2)^{3/2}] \tag{6}$$

with constraints

$$\zeta_c = \gamma - [\Omega\gamma(1-\alpha)\cdot(1-\beta^2)]^{1/2} > 0 \tag{6a}$$

$$\rho_H = \beta\left\{1 + \frac{2}{\beta^2}\left[\frac{\gamma}{\Omega}(1-\alpha)\cdot(1-\beta^2)\right]^{1/2}\right\}^{1/2} < 1 \tag{6b}$$

Type 3: $\zeta_c < 0$, $\rho_H = 1$

$$A_3 = \frac{2}{3\Omega^2(1 - \beta^2)}[(1 + \Omega^2)^{3/2} - (1 + \Omega^2\rho_0{}^2)^{3/2}] \tag{7}$$

with constraints

$$\zeta_c = -\frac{\Omega}{2}\left\{1 - \beta^2 - 2\left[\frac{\alpha\gamma}{\Omega}(1 - \beta^2)\right]^{1/2}\right\} < 0 \tag{7a}$$

$$\rho_H = \left[\frac{2\gamma}{\Omega} + 1 - 2\left[\frac{\alpha\gamma}{\Omega}(1 - \beta^2)\right]^{1/2}\right\}^{1/2} > 1 \tag{7b}$$

$$\beta < \rho_0 = \left\{1 - \left[2\frac{\alpha\gamma}{\Omega}(1 - \beta^2)\right]^{1/2}\right\}^{1/2} < 1 \tag{7c}$$

Type 4: $\zeta_c < 0$, $\beta < \rho_H < 1$

$$A_4 = \frac{2}{3\Omega^2(1 - \beta^2)}[(1 + \Omega^2\rho_H{}^2)^{3/2} - (1 + \Omega^2\rho_0{}^2)^{3/2}] \tag{8}$$

with constraints

$$\zeta_c = -\frac{1}{2}\{\Omega[1 - (1 - \alpha)\cdot(1 - \beta^2)] - \gamma\} < 0 \tag{8a}$$

$$\rho_0 < \rho_H = \left[\frac{\gamma}{\Omega} + 1 - (1 - \beta^2)\alpha\right]^{1/2} < 1 \tag{8b}$$

$$\beta < \rho_0 = \left[1 - (1 - \beta^2)\alpha - \frac{\gamma}{\Omega}\right]^{1/2} < \rho_H \tag{8c}$$

When $\beta = 0$, no core in the rotor, all the equations reduce to the expression given in Ref. *1*, p. 178.

NUMERICAL RESULTS

A Fortran program for an IBM/360 series digital computer was written to calculate the reduced paraboloid interfacial area A_i as a function of speeds of revolution and the loading levels of liquid. By use of Eqs. (5)–(8), the reduced paraboloid interfacial area was calculated for K-III and J-I rotors; the results are presented in Figs. 2 and 3. The dimensions of these rotors are listed in Table 1.

From Figs. 2 and 3 it is found that the variation of the reduced paraboloid interfacial area as a function of both speeds of revolution and

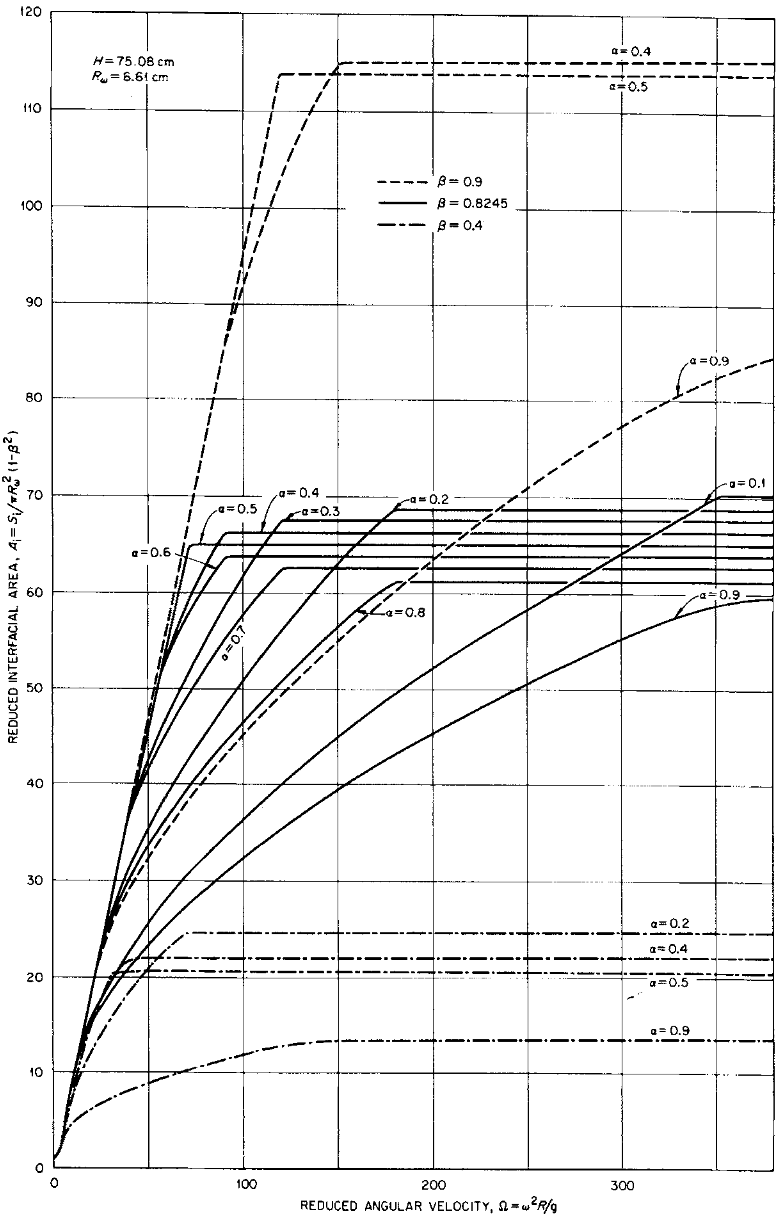

FIG. 2. Variation of reduced interfacial area with respect to speeds of revolution for the K-111 rotor.

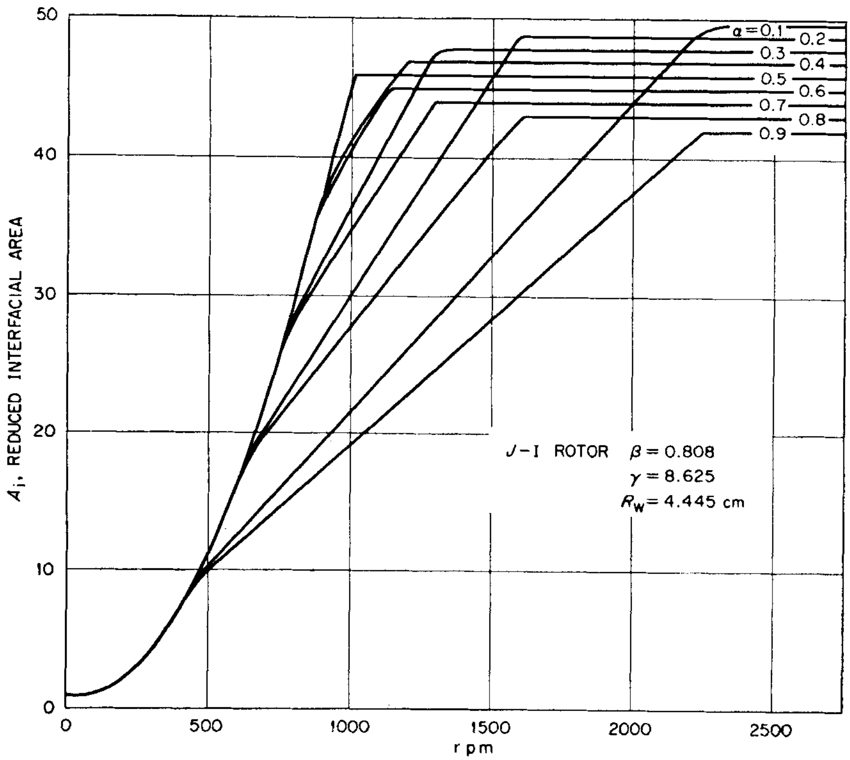

FIG. 3. Variation of reduced interfacial area with respect to speeds of revolution for the J-1 rotor.

TABLE 1

Dimensions of Rotors

Dimension (cm)	K-111	J-1
Height, H	75.08	38.338
Rotor diameter, R_w	13.22	8.890
Core diameter, R_c	10.90	7.184

the loading levels of liquid exhibits the same general profiles as the rotor without core. Therefore the variation with respect to $\gamma[= H/R_w]$ for rotors with core is expected to be the same as rotors without core. Hence the variation of the paraboloid interfacial area with respect to γ has not been performed.

During the gradient reorientation from rest to a stable orientation in a high centrifugal force field, the shearing forces occurring in a liquid confined in a closed cylinder will cause an increase in dispersion of a reorienting gradient system. The dispersion coefficient contributed from reorientation, D_{orien}, may be written as

$$D_{\text{orien}} = \frac{dS}{dt}\left[\frac{\text{area}}{\text{time}}\right] \tag{9}$$

In a given time period the dispersion due to reorientation shearing forces is

$$\sigma = \int_0^t D_{\text{orien}}\, dt = \int_0^t \frac{dS}{dt}\, dt = S(t) - s(0) \tag{10}$$

Investigating Figs. 2 and 3, one finds that an isodensity interfacial area will approach a constant value (completely oriented) after a certain rotational speed for a given liquid loading level. A rotational speed, rpm $= (60 \times \omega)/2\pi$, is directly proportional to an angular velocity $\omega[= \sec^{-1}]$. Thus Eq. (10) may be rewritten

$$\begin{aligned}\sigma &= \int_0^t \frac{ds}{dt}\, dt = \int_0^{t_c} \frac{ds}{dt}\, dt + \int_{t_c}^t \frac{ds}{dt}\, dt = \int_0^{t_c} \frac{ds}{dt}\, dt = S(t_c) - S(0) \\ &= \int_0^{\omega_c} \frac{ds}{d(1/\omega)}\, d\left(\frac{1}{\omega}\right) = \int_0^{\omega_c} \frac{ds}{d\omega}\, d\omega = S(\omega_c) - S(0)\end{aligned} \tag{10a}$$

in which t_c is the time required to reach a completely reoriented paraboloid configuration, and ω_c is the angular velocity a which the paraboloid configuration is completely reoriented. From Eq. (10), one may see that $S(\omega_c)$ is a function of rotor configuration and liquid loading level only. Therefore we conclude that dispersion from a reorienting gradient system is independent of rate of acceleration; it is a constant depending on rotor configuration and liquid loading levels.

For evaluation of dispersion constants for K-III and J-I rotors with variation of core radius ($0 < \beta < 1$) and of reduced liquid loading level, α varying from 0.1 to 0.9, a graphical differentiation and integration was performed from Figs. 2 and 3. The dispersions due to reorienting for

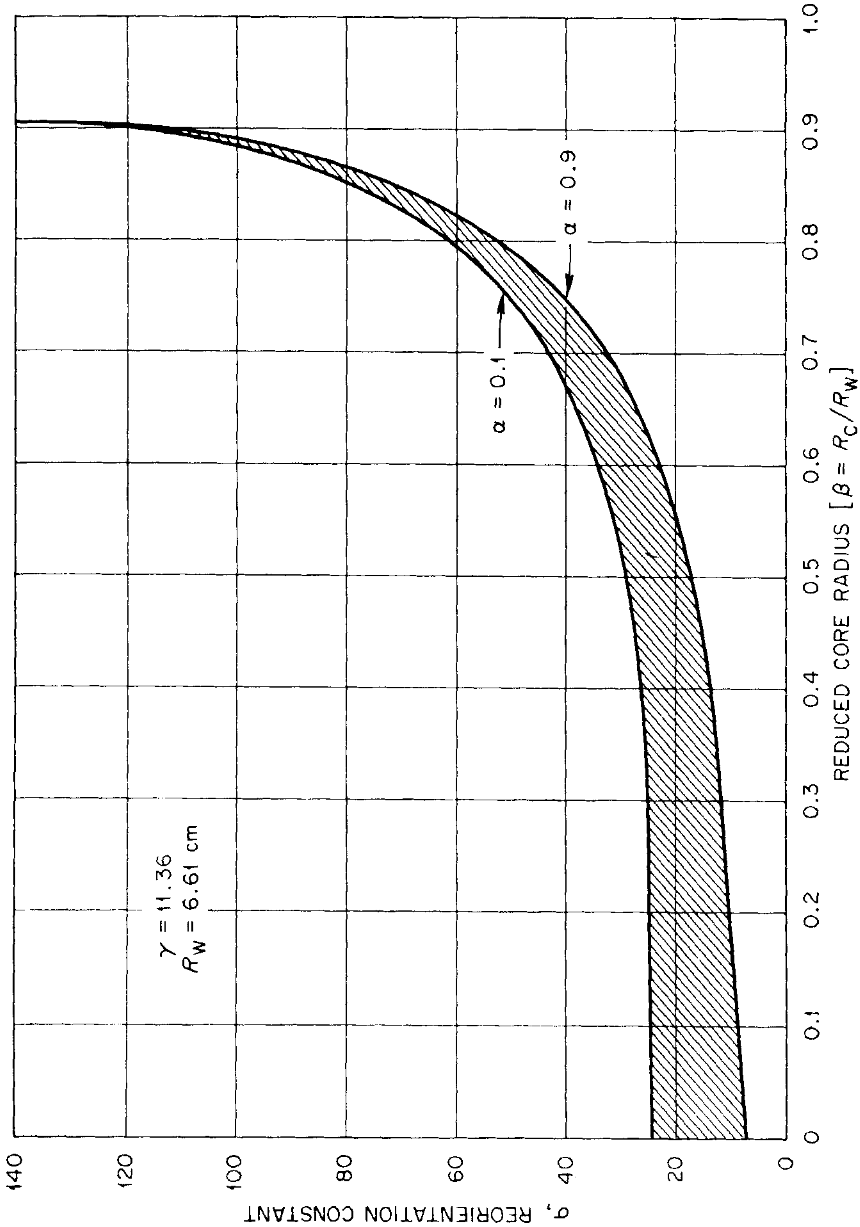

FIG. 4. Calculated dispersion constants as a function of annular gap (β) in rotor for K-111.

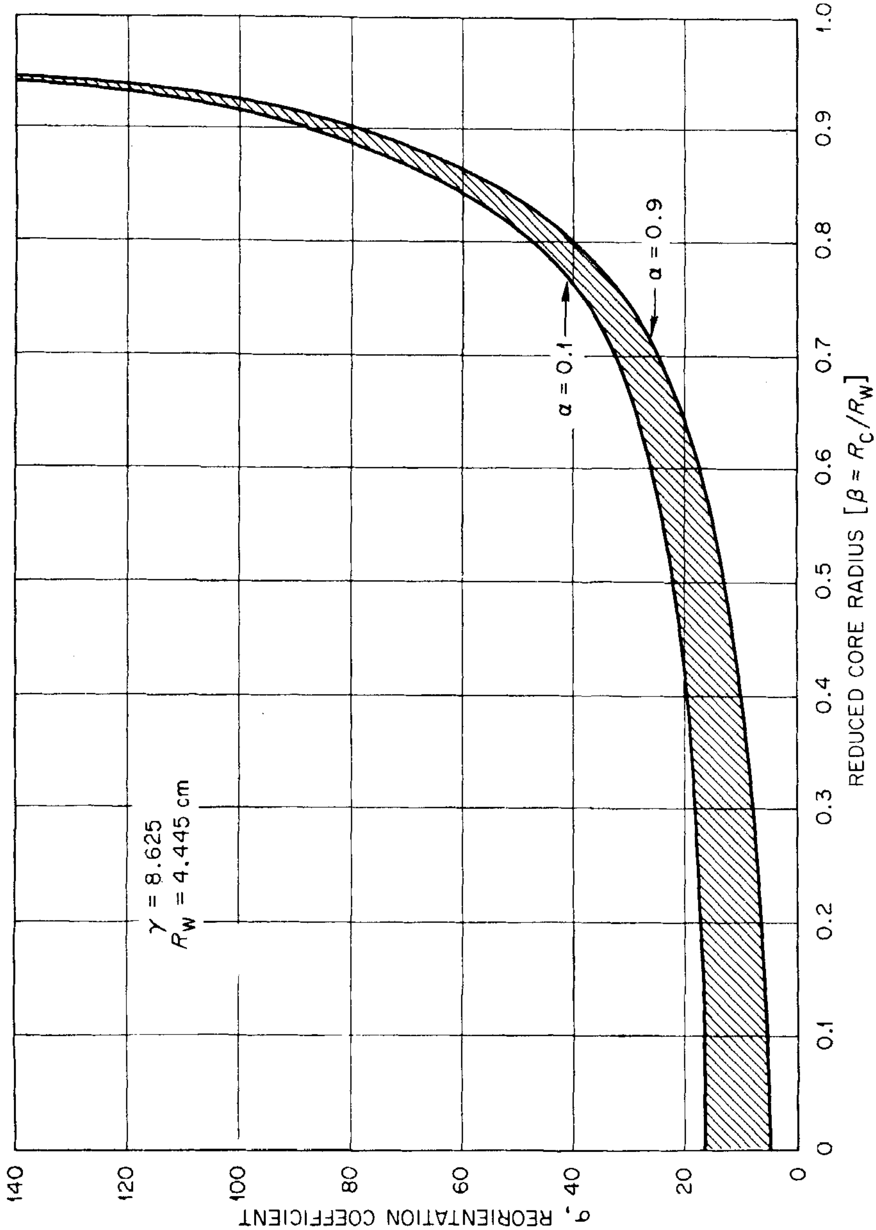

FIG. 5. Calculated dispersion constants as a function of annular gap (β) in rotor for J-1.

K-III and J-I rotors are presented in Figs. 4 and 5, respectively, in a unit of number of times the isodensed area increased.

DISCUSSION

From the foregoing analysis we would like to make the following suggestions: One should accelerate a rotor quickly to reduce total operation time, so that dispersion due to molecular diffusion will be minimized (*3*). Control of rotor acceleration or deceleration is a very difficult task. Therefore the control is unnecessary. Furthermore, at high speeds the fluctuation of rotor speed is less than at lower speeds and a smooth operation is easier to obtain. This finding is in agreement with our experimental investigations (*4*) on two-dimensional transient flow pattern and shear stress distributions, in which we have found that changing the rate of acceleration produces no noticeable effect in any flow patterns, shear stress distributions, or their magnitudes during transient periods for a given rotor.

We feel that the improvement of zonal centrifugation should be directed to an improvement in loading and unloading methods to reduce the dispersion from these operations. The next step will be to improve rotor configuration so that dispersion from shearing force by the reorienting gradient can be minimized.

SYMBOLS

A	reduced paraboloid interfacial area, defined in Eq. (4i)
d	liquid loading level (cm)
g	acceleration of gravity (980 cm/sec^2)
H	height of rotor (cm)
r	radius coordinate
r_H	radius of isodense paraboloid at top wall (cm)
r_0	radius of isodense paraboloid at bottom wall (cm)
R_c	outside radius of core (cm)
R_w	inside radius of rotor (cm)
S_i	paraboloid interfacial area of type i (cm^2)
V	volume of liquid (cm^3)
Z	vertical axial coordinate
Z_0	minimum of the height of isodense paraboloid (cm)
Z_c	height of isodense paraboloid at core (cm)
Z_w	height of isodense paraboloid at rotor wall (cm)
α	reduced liquid loading level, defined in Eq. (4a)

β ratio of core radius to rotor wall, defined in Eq. (4b)
γ ratio of height to rotor wall, defined in Eq. (4c)
ρ_H reduced radius of isodense paraboloid at top wall, defined in Eq. (4d)
ρ_0 reduced radius of isodense paraboloid at bottom wall, defined in Eq. (4e)
ζ_c reduced height of isodense paraboloid at core, defined in Eq. (4f)
ζ_0 reduced minimum height of isodense paraboloid, defined in Eq. (4g)
ω angular velocity ($\sec^{-1}$)
Ω reduced angular velocity, defined in Eq. (4h)

Subscripts

0 quantity evaluated at minimum position or at bottom wall
1, 2, 3, 4 classification of paraboloid type
c quantity evaluated at core wall
H quantity evaluated at top wall
w quantity evaluated at rotor wall

Acknowledgments

The author wishes to express his deep appreciation to Dr. N. G. Anderson, Director of Molecular Anatomy (MAN) Program, Oak Ridge National Laboratory, for his constant encouragement; to Mr. R. A. Carter who computed the isodensity interfacial areas; and to Mr. R. K. Genung, of the University of Tennessee, for much valued assistance. The partial financial support of NSF Grant GK-11378 is gratefully acknowledged.

REFERENCES

1. H. W. Hsu and N. G. Anderson, *Biophys. J.*, *9*(2), 173 (1969).
2. R. B. Bird, W. E. Steward, and E. N. Lightfoot, *Transport Phenomena*, Wiley, New York, 1960, p. 98.
3. R. K. Genung and H. W. Hsu, *Separ. Sci.*, *7*(3), 249 (1972).
4. H. D. Pham and H. W. Hsu, *Ind. Eng. Chem., Process Des. Develop.*, *11*, 556 (1972).

Received by editor February 23, 1973